The eROSITA Bulletin
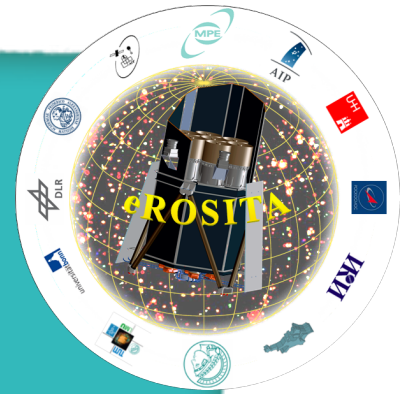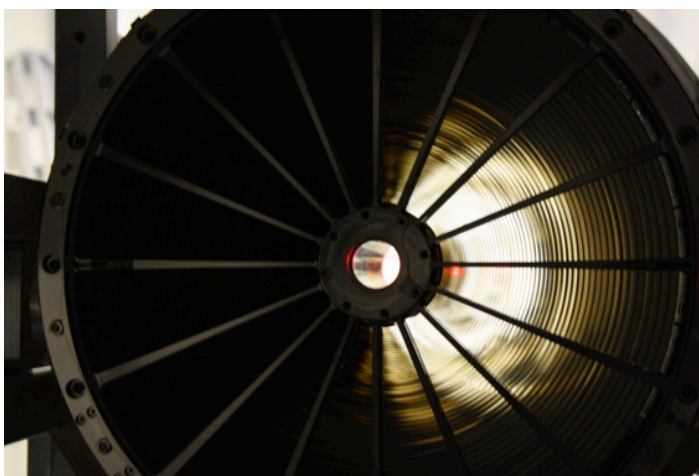
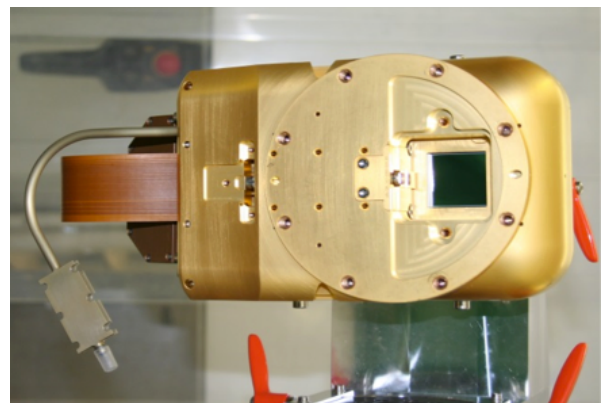## 1. Project status and milestones

The complete Mirror Module FM4 in the PANTER facility during alignment measurement with auto-collimation

Mission timeline: The preparation of the Spektrum Roentgen Gamma (SRG) mission advances on all fronts. Huge progress has been made in the last six months, but, at the same time, bottlenecks in the various production and testing chains were identified, leading to a revised schedule. According to the latest plan, eROSITA will be delivered in June 2015, ART-XC in August of the same year, for a foreseeable SRG launch in December 2015/January 2016. The official SRG status meeting was held on February 5 at GSOC, in Oberpfaffenhofen, near Munich, in coincidence with the meeting of the Radiocomplex review team. More about this in the next issue of the Bulletin.

2. Camera development

*The eROSITA QM (Qualification Model) camera*

Camera electronics: The engineering model of the camera electronics has recently been completed and successfully tested together with the qualification model (QM) of the pn-CCD camera. We measured a FWHM of 136 eV for the Mn-Kα line at 5.9 keV, which meets the eROSITA requirement value (see figure on next page). The camera was also exposed to vibration tests on the shaker of MPE, and no damage occurred as proven in the subsequent tests.

Warm test of camera assembly: During several qualification steps, and before launch in Baykonour, there is no possibility to evacuate the camera for cooling of the sensor chip. So-called 'warm tests' can be carried out to check the functionality

of the camera system and get necessary information about the read noise of the detector. A few months ago, we successfully performed the first warm test with the complete camera assembly.
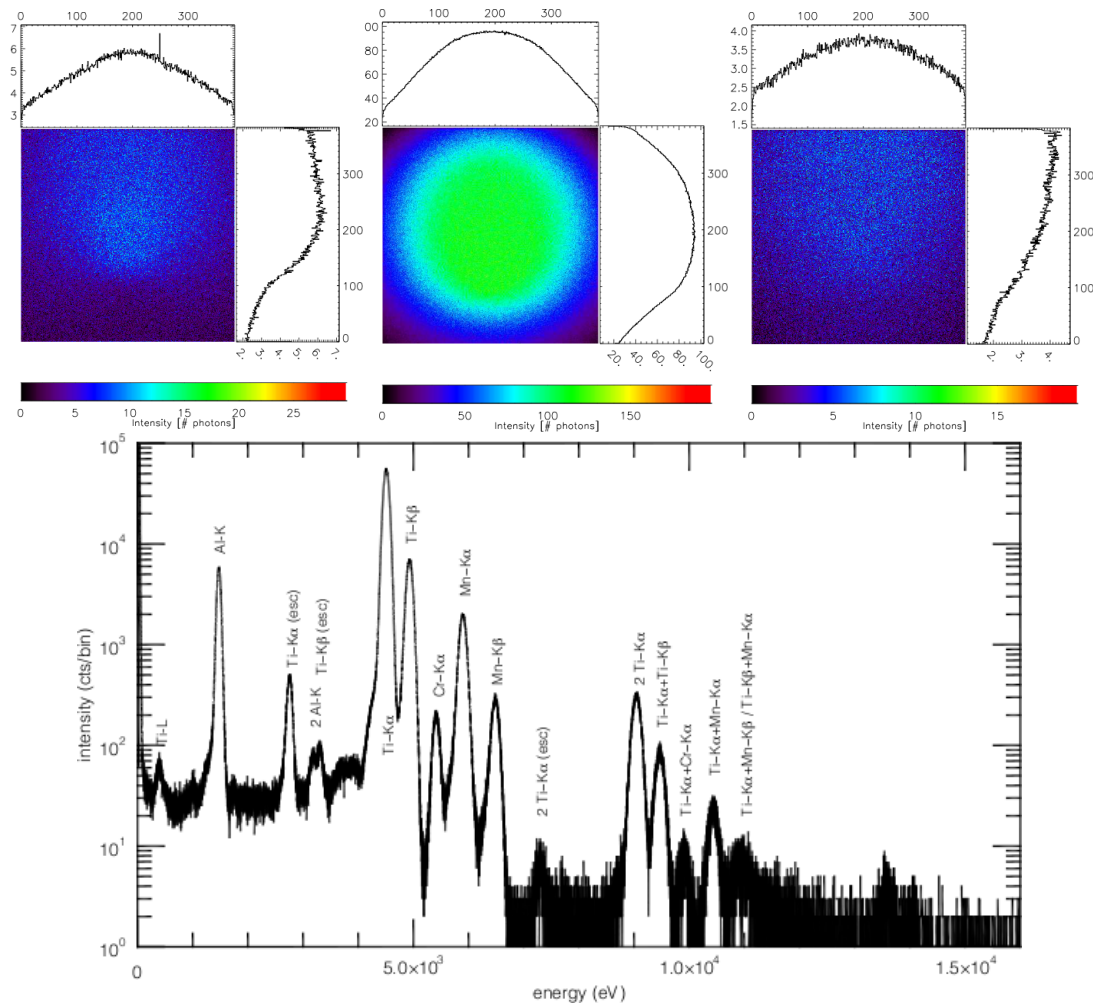
Bottom: Spectrum emitted by on-board calibration source and measured with the QM camera. Notice the wide energy range covered by the detectable emission lines. The three intensity images on the top show that all three main calibration source lines (Al-Kα, Ti-Kα, Mn-Kα, from left to right) fully illuminate the entire CCD image area as needed for optimum calibration on-board.

Operation of complete camera assembly under nominal conditions: While all previous performance measurements so far were carried out in the small GEPARD test chamber, we transferred the camera assembly to the 10m large PUMA facility at MPE for further system tests. There, the complete camera assembly is operated in vacuum. Such a configuration allows to test the on-board calibration source (^{55}Fe source with Al-Ti target), which is needed in space in order to correct the degrading charge transfer efficiency of the CCD during the mission. During this campaign, we also performed thermal vacuum and spectroscopic tests of the detector by exposing it to various X-ray fluorescence energies (see figure above). Due to the relatively short decay time of the calibration source (2.7 years 1/2 time), the ones for flight system will be purchased at the last possible time before integration.

Flight detector FM1: The assembly of the first flight detector has meanwhile started.

Reference: Meidinger et al., Progress of the X-ray CCD camera development for the eROSITA telescope, Proc. of SPIE, Vol. 8859, 2013

3. Status of eROSITA Mirror Assembly

Each Mirror Assembly (MA) consists of two main parts: (i) the Mirror Module itself, with 54 nested shells, and (ii) an X-ray baffle on top of it, which reduces the stray-light originating from single reflections. On the basis of the imaging performance tests, seven out of the existing eight MA will eventually be integrated into the telescope, while one will serve as spare. The last module was completed by Media Lario in mid-November 2013. The eight X-ray baffles were manufactured at MPE and completed by the end of October 2013. By mid-December 2013, all Mirror Modules had been acceptance-tested.

Mirror Module Acceptance Tests: The main goal of the acceptance tests was to verify the optical performance after delivery of the Mirror Modules. The performance criteria were: point spread function (PSF) and effective area, both for different photon energies, alignment, and focal length. The X-ray tests were performed in the big vacuum chamber of MPE's X-ray test facility PANTER. A target source was used to illuminate the Mirror Modules with monochromatic light of the C-Kα line (0.27 keV), the Al-Kα line (1.49 keV), the Cu-Kα line (8.04 keV) and occasionally with characteristic lines of other elements. The focal lengths were measured with a calibrated mechanical-optical gauge after venting the vacuum chamber. The alignment of the X-ray optical axis was measured w.r.t an optical reference mirror in the centre of the mirror module's spider wheel using an auto-collimator. A successful acceptance test was a necessary condition to proceed with the next step, i.e. the mounting and alignment of the X-ray baffle. Mirror module FM1 was the first to be completed, and was subject to an extended sequence of tests: acceptance was followed by a performance test with the X-ray baffle mounted and by further performance checks after each environmental test. FM1 was also part of the "telescope module test", where it was tested under space conditions together with other components, such as thermal baffle, electron deflector, optical bench, and filter wheel. All MAs will be calibrated with a procedure similar to the acceptance test. This will take place in the course of 2014.

	Specification		Acceptance Test							
	Orbit	Derived for PANTER	FM 1	FM 2	FM 3	FM 4	FM 5	FM 6	FM 7	FM 8
			Dec 2012 / Jan 2013	Mar 2013	May 2013	Sep 2013 / Oct 2013	Sep 2013	Dec 2013	Dec 2013	Jun 2013
HEW Al-K (1.49 keV)	< 15″	< 15″	16.1″±0.2″	16.8″±0.3″	15.7″±0.3″	16.0″±0.3″	16.2″±0.2″	16.3″±0.3″	15.6″±0.3″	17.1″±0.3″
HEW Cu-K (8.04 keV)	< 20″	< 20″	15.2″±0.1″	15.4″±0.3″	16.7″±0.4″	16.4″±0.3″	16.2″±0.3″	16.2″±0.3″	16.6″±0.3″	18.4″±0.4″
W90 C-K (0.28 keV)	< 90″	< 90″	~89.8″	~106.5″	~107.9″	~106.7″	~119.6″	~127.3″	~107.9″	~123.6″
Eff. Area[1] Al-K	> 350 cm²	> 363.6 cm²	391.9 cm² ± 16.1 cm²	391.1 cm² ± 20.6 cm²	392.6 cm² ± 15.5 cm²	369.4 cm² ± 24.8 cm²	387.9 cm² ± 19.2 cm²	378.4 cm² ± 19.2 cm²	391.6 cm² ± 24.8 cm²	389.6 cm² ± 20.5 cm²
Eff. Area[1] Cu-K	> 20 cm²	> 21.0 cm²	24.8 cm² ± 0.8 cm²	24.8 cm² ± 1.1 cm²	25.1 cm² ± 1.2 cm²	23.8 cm² ± 0.9 cm²	24.1 cm² ± 0.6 cm²	25.1 cm² ± 1.1 cm²	25.0 cm² ± 0.9 cm²	24.2 cm² ± 1.0 cm²
Micro-roughness	< 0.5 nm	Scattering Cu-K < 15.7%	Scattering Cu-K 10.8%	Scattering Cu-K 11.2%	Scattering Cu-K 10.7%	Scattering Cu-K 12.0%	Scattering Cu-K 13.3%	Scattering Cu-K 11.3%	Scattering Cu-K 11.7%	Scattering Cu-K 11.4%
Focal length	1600±10 mm	1600±10 mm (with lens equation)	1600.94 ±0.5 mm	1600.90 ±0.5 mm	1600.77 ±0.5 mm	1600.93 ±0.5 mm	1601.14 ±0.5 mm	1601.80 ±0.5 mm	1600.93 ±0.5 mm	1601.21 ±0.5 mm
Optical axis alignment	< 30″	< 30″	0″±21″	30″±14″	110″±14″	47″±14″	72″±14″	61″±14″	38″±14″	105″±14″

*Summary of Mirror Modules performance in the acceptance tests*

The general result from the acceptance test is that most of the specifications are met; the only exception is the low energy on-axis angular resolution (16.2″ HEW on average) and slightly above the W90 of 90″ (see Table above).

Telescope defocusing tests: In the all-sky survey the average angular resolution is not only driven by the on-axis HEW, but also by the off-axis blurring which is intrinsic to Wolter-type optics. The PSF of the eROSITA telescopes degrades with increasing off-axis angle from ~16" (HEW) on the optical axis to ~76" at the edge of the field of view. This is partly due to the curved focal plane of the telescope optics (see Figure below).
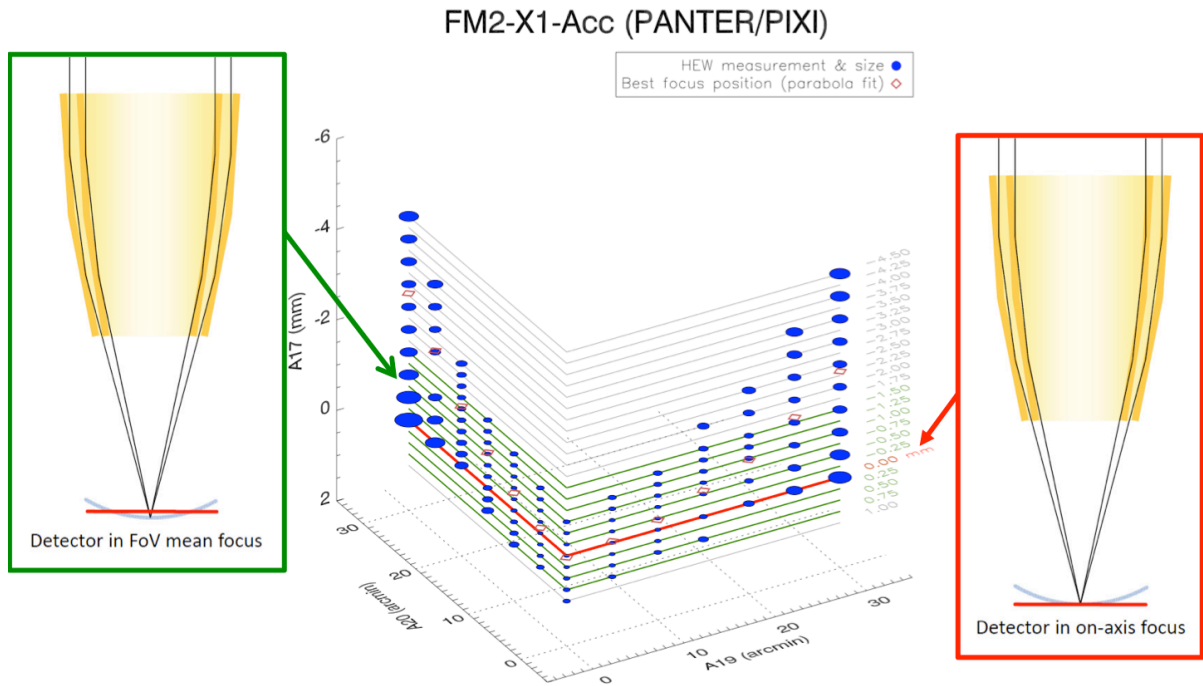

PSF size of a mirror for different positions of the detector, measured at PANTER. The vertical axis is the optical axis. The red plane is the detector plane position "in-focus" (see illustration on the right), all other planes correspond to subsequent 0.25 mm shifts along the optical axis (see illustration on the left). Each circle is proportional to the HEW size, the best-focus being the red losanges. The plot clearly illustrates the curved nature of the mirror focal plane (V. Burwitz, N. Clerc, K. Dennerl, G. Hartner, B. Menz).

We have measured the PSF at various intra-focal shifts of the detector and calculated the FoV average. The Figure on the right shows the measured on-axis resolution and the calculated average resolution in the 61 arc minute field-of-view, for both "no shift" and for a test-case of a 0.4mm shift. While the on-axis resolution degrades by about 2", the average resolution improves by more than three arc seconds. On the basis of these tests, the current baseline for the detector position foresees a 0.4 mm intrafocal shift.
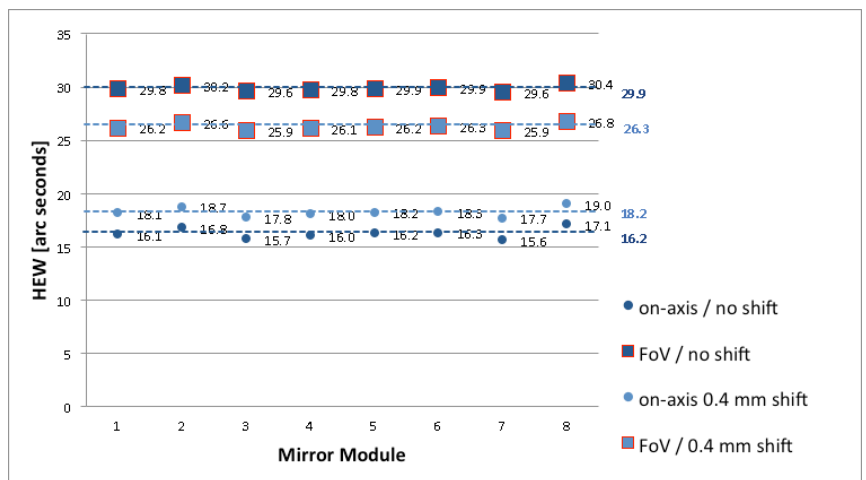
Angular resolution on-axis and FoV average – both for in-focus position and 0.4 mm intrafocal

Alignment and Integration of X-Ray Baffles: During the manufacturing of the X-ray baffles, all shells were roundness-measured. Deviations from perfect shape cause loss of effective area by shadowing the mirrors, and less efficient blocking of stray-light. These effects were quantified by analysis of all roundness measurements. The results indicate that stray-light reduction will be between 91% and 92% (with a perfectly designed baffle blocking 95% of stray-light), for a loss of collective area of about 2.4%. The completed X-ray baffles have been successively mounted on the Mirror Modules, the last one in early February 2014. A dedicated alignment stand has been built in order to accomplish the precise positioning of the X-ray baffle shells w.r.t. the mirror shells. This requires alignment in all six degrees of freedom. In particular, the lateral position has to be satisfied by better than 20 μm (in fact, an accuracy of about 10 μm was achieved). The alignment itself is done with fine pitch threads, while the criteria for the correct positioning come from optical monitoring. For this purpose a telecentric lens with an image ratio of 1:10, a high resolution CMOS camera and bright and homogenous illumination were needed.
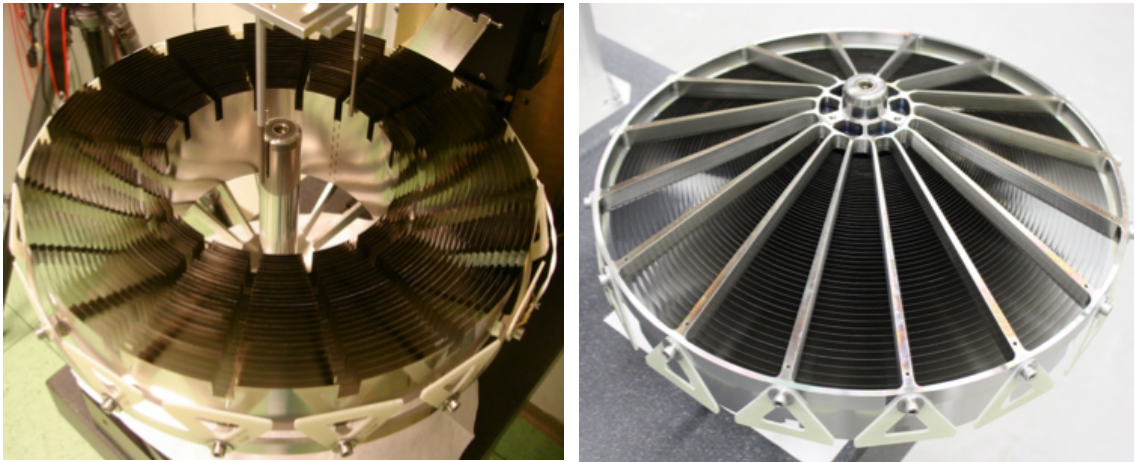

X-ray baffle during manufacturing (left) and immediately before mounting on the mirror module (right)

4. Ground Segment and Operations

Data analysis software: Integration and testing of the data processing pipeline is ongoing. Core components of the data analysis software (energy calibration, exposure map creation, source detection, extraction of spectra and light curves) are available in functioning versions and were demonstrated at the consortium meeting. Coding is proceeding in several areas (MIP exposure correction, attitude handling, source specific products); see the adjoining figure for a breakdown of the status of the software tasks comprising the eROSITA science analysis software (**green:** testing, **amber:** coding, **gray:** design). Performance characterization of the eROSITA source detection software is underway; see the following paragraph for some recent results. The eROSITA ground software is created by a team of developers at MPE, AIP, Remeis-Sternwarte Bamberg, Hamburger Sternwarte, MPA, AIfA, and the National Observatory of Athens.

Status of eROSITA-SASS tasks (pipeline & interactive)

TEL chain		EXP chain		DET chain	
EVPREP	✓	EXPMERGE	✓	ERMASK	✓
EXPOSURE	✓	RADEC2XY	✓	ERBACKMAP	✓
FTFINDHOTPIX	✓	FLAREGTI	✓	ERSENSMAP	✓
PATTERN	✓	BINIMAGE	✓	ERBOX	✓
ENERGY	✓	EXPMAP	✓	ERMLDET	✓
BCKGRND	✓			**SOU chain**	
ATTPREP	✓	**Preprocessor**			
TELATT	✓	TM2FITS	✓	SRCTOOL	✓
EVATT	✓	PREPROC	✓	CATPREP	✓
MKFILTER	✓			SPECFIT	✓
TELGTI	✓	**Pipeline control**		VARICHCK	✓
TELSELECT	✓	EROPIPE	✓	DPVALP	✓
TELSTAGE	✓	PREXEC	✓	DPVALV	✓
		PROC	✓	CATINGEST	✓

Optimizing the detection sensitivity as a function of detector focus offset: As we discuss above, it is possible to improve the field-averaged PSF by shifting the detectors towards the telescopes at the expense of a slight blurring of the PSF on the optical axis. Since any focus offsets of the detectors have to be fixed before launch, a careful assessment of the impact on the instrument performance is needed. We performed simulations of 20 survey fields with a total area of 200 square degrees. Each field was simulated for 5 focus shifts between 0.0 and 0.6 mm and processed with the eROSITA-SASS source detection pipeline, employing box detection and PSF fitting algorithms. The pipeline was applied in two different variants: 1) binning of photons from the entire FoV into one image, and 2) separation of near-axis and off-axis (> 16') photons into separate images, which were then simultaneously processed by the detection software. Correlation of the resulting source lists with the input catalogues of AGN and extended sources gives the following results:
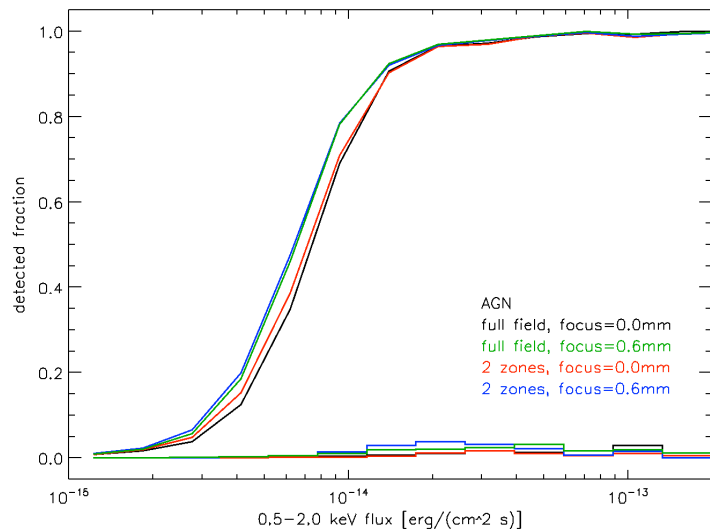

Point source detection probability at 2 ksec survey exposure as a function of source flux for different focus shifts and detection methods; the fraction of AGN incorrectly detected as extended is displayed at the bottom of the figure (G. Lamer, AiP).

- Shifting the focus from the nominal position significantly improves the survey sensitivity for both point sources and extended sources. The best sensitivities are reached for the largest simulated focus shifts.
- Using separate images for on-axis and off-axis photons slightly improves the detection sensitivity, also in combination with focus shifts. However, this software setting cannot be regarded as replacement for the focus optimization, since its effect is clearly smaller.
- The potential improvement in sensitivity is quite significant. For a survey exposure of 2 ksec the limiting flux is pushed lower by about 15% ,the total number of detected point sources increases by 10-20% when applying both a focus shift and the modified detection method (see Figure above).

Mission planning, interaction with Russian team: The eROSITA_DE mission planning team discussed and coordinated data formats for exchanging mission planning information, covering all mission phases and observing modes, with their Russian counterparts. An updated L2 orbit for the SRG mission was provided by the Russian colleagues (see figures by J. Robrade on the next page; orbit data by Applied Math. Inst., Moscow, obtained via Igor Lapshov, IKI; Earth not to scale). Optimization of mission planning strategies considering different SRG antenna concepts, including tests for the creation of mock timelines covering the initial mission phases, are underway.

Catalog database: With help from the MPA Galformod team and the IPP computer center (RZG) a trial version of the Skynode multi-lambda catalog database (provided by Alex Szalay, JHU) was installed at IPP and is currently undergoing testing. We are exploring various options to interface the database with existing and to be developed frontends in the context of the eROSITA project.

External technical collaboration: Ioannis Georgantopoulos and Nikos Nikoloudakis of the National Observatory of Athens joined the eROSITA software team as external technical collaborators of
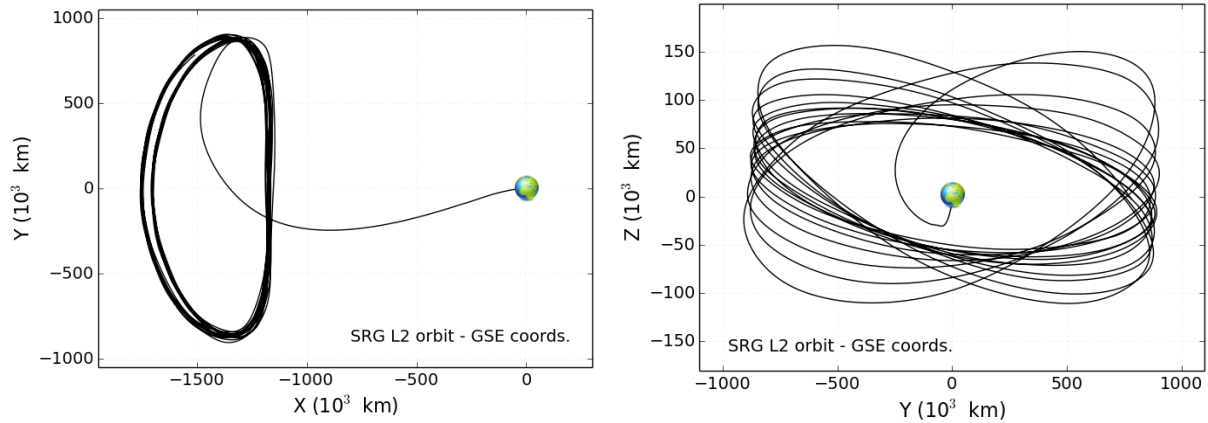
*Planned orbit of SRG in the XY (left) and YZ (right) projections. The X axis is the sun-earth direction.*

the eROSITA_DE consortium. They will contribute to the eROSITA science analysis software development, initially providing software for PSF modeling and exposure correction.

Management: The eROSITA software team moved its internal discussions, including a system for tracking software changes and problem reports, to the AWOB collaboration tool (Astronomers WOrk Bench). AWOB is a project of the Max-Planck Digital Library, MPA, and MPE.

5. Multi-wavelength surveys and follow-up preparation

DES Science Verification: Photo-z: The first season observations from DES, over an area of ~2500 deg^2 of eROSITA-DE sky, are now just ending. Meanwhile, the Science Verification data from last year is feeding several cluster analyses relevant to eROSITA. Christina Hennig (LMU) is completing a DES study of 85 SPT selected massive clusters extending over the full eROSITA cluster redshift range of interest. With this study she has been able to characterize the galaxy populations over this full redshift range in clusters with $M_{200} > 3 \times 10^{14}$ M$_\odot$ and to demonstrate a characteristic single cluster photometric redshift accuracy of $\delta z/(1+z)$ =0.016. Photometric redshifts of this accuracy meet the requirements needed to pursue the eROSITA cluster cosmology experiment that relies on the cluster mass function evolution. The precise understanding of the galaxy population evolution that arises from this study will enable us to quantify the process of optical confirmation of the eROSITA clusters within this mass range. We will use this information to build a model of the eROSITA cluster X-ray selection and optical confirmation, which is then a critical input to the cosmological analysis of the sample.
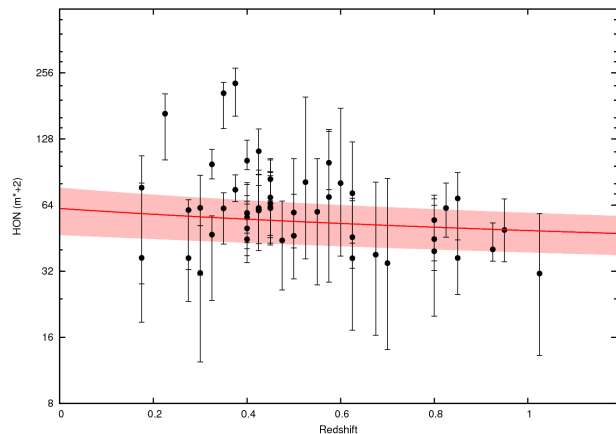
The number of galaxies (PRELIMINARY) brighter than m*+2 (corrected to 5x10^{14}M$_\odot$ using the HON trend with mass) as a function of redshift for DES observations of SPT selected clusters. The detailed characterization of the cluster galaxy population as a function of redshift and mass will inform the eROSITA cluster followup and cosmological studies (C. Hennig/LMU)

Stacked tangential and cross shear profile
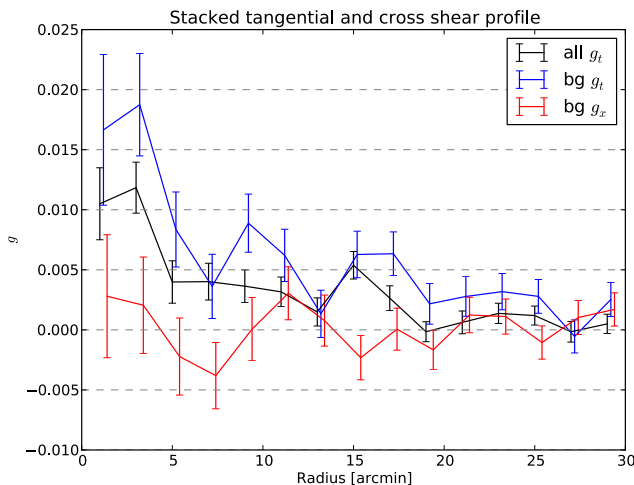
DES blinded weak lensing shear profiles (PRELIMINARY)) from an r band stack of 45 SPT selected clusters extending to z~0.8. The red curve contains the cross-shear, consistent with zero throughout. The blue one contains source galaxies between $z_{cl}+0.2<z_{src}<1.5$, and the black all galaxies (D. Gangkofner, J. Dietrich/LMU and the DES weak lensing SWG)

DES Science Verification: Weak lensing: Within DES weak lensing analyses of SPT selected clusters are proceeding. Initial results from a stacked profile appear in the figure below. These profiles use im3shape measurements from sources with SNR>10 extracted from the r band imaging. Stacked profiles over 45 clusters are shown, with the cross-shear (red) being consistent with zero (a check on catalog systematics), the full galaxy sample (black) showing a strong detection, and the background or source galaxy sample (blue) showing the strongest detection. The source galaxies were selected using photo-z's to lie behind the cluster. These initial tests using DES-SV data are encouraging, delivering useable shear measurements for about 12 galaxies/arcmin^2 over the full redshift range. At this source density, it will be possible to extract robust single cluster masses for the massive eROSITA clusters out to z~0.3 and to use stacking techniques like those applied to the SPT sample to constrain the ensemble masses of clusters at higher redshift and at lower mass.
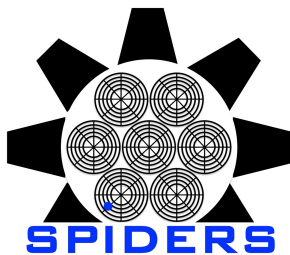
SPIDERS gets green light: Last December 12-13 in Berkeley, California, three extragalactic surveys planned for the next, fourth, generation of the SDSS underwent a critical review. eBOSS (extended Baryon OScillation Survey), TDSS (Time Domain Spectroscopic Survey) and SPIDERS (Spectroscopic IDentification of ERosita Sources) were all given green light for a start next July 2014, with a number of suggestions for optimization.

The main goal of SPIDERS will be to provide a complete and homogeneous optical spectroscopic follow-up of X-ray sources (both point-like and extended) that will be detected by eROSITA in its first two years of survey operation over the largest possible area within the "German" eROSITA sky accessible by SDSS. As the eROSITA data will only become available in the last three years of SDSS-IV, the SPIDERS survey will be executed in three steps, corresponding to three different (increasing) levels of allocated fiber density, with the shallower early phases dedicated to the follow-up of all ROSAT All-sky Survey (RASS) sources still missing spectroscopic follow-up within the full eBOSS footprints (7500 deg^2). Eventually, SPIDERS will obtain ~60,000 spectra of ROSAT and eROSITA X-ray selected AGN, about 40% of which in common with the eBOSS optical QSO survey and the remaining (thus ~35,000) unique SPIDERS AGN targets. This spectroscopic X-ray selected sample will be 4 times larger than the total number of X-ray AGN with spectroscopic redshift currently known, and about a factor 20 larger than any existing coherent, contiguous, well defined, X-ray survey.

As far as clusters of galaxies are concerned, the first, shallower, tier, before eROSITA data become available, will be devoted to the study of 3,000 clusters from RASS, PLANCK and XCLASS. Subsequently, the complete follow-up of 3,000 eROSITA X-ray detected clusters and groups of

galaxies will be used to determine absolute parameters (X-ray luminosity, total mass) for the brightest and more massive objects discovered in eRASS. The combined sample will enable cosmological parameters estimations, thanks to the leverage clusters provide on the growth rate of structures, significantly better than with any existing cluster survey to date.

In order to do so, SPIDERS will take spectra of 40,000 red-sequence galaxies contained within those clusters, thus providing a unique view of galaxy evolution in the densest environments of the cosmic web.

6. Prospects for Large Scale Structure and BAO studies

The eROSITA all-sky survey will produce an unprecedented sample of about 3 million X-ray selected AGN. With the median redshift of $z \approx 1$ and a typical luminosity of $\sim 10^{44}$ erg/s, about 40% of eRASS objects will be located between redshifts $z=1$ and $z=2$ (Kolodzig et al. 2013a). About 10^4-10^5 AGN will be located beyond redshift $z=3$ and $\sim 2{,}000$-$30{,}000$ AGN beyond $z=4$, the exact number depending on the behavior of the AGN XLF in the high redshift and luminosity regimes.

With such a large AGN sample it will become feasible for the first time to perform detailed studies of AGN clustering as a function of redshift and AGN luminosity (Kolodzig et al. 2013b). This, in combination with our good understanding of the evolution of the underlying large-scale matter distribution, as traced by the dark matter halos, opens up a way to study AGN evolution in the general framework of cold dark matter cosmologies. In particular, one expects to gain substantial insights into AGN triggering mechanisms, their evolution as a function of cosmic environment along with a detailed mapping of the supermassive black hole activity throughout cosmic history.

These studies do not require detailed redshift information and can already be performed with moderately accurate photometric redshifts. However, with full (spectroscopic) redshift information available, the AGN sample provided by eROSITA can be turned to a powerful cosmological probe by measuring baryonic acoustic oscillations (BAOs) with high statistical significance.
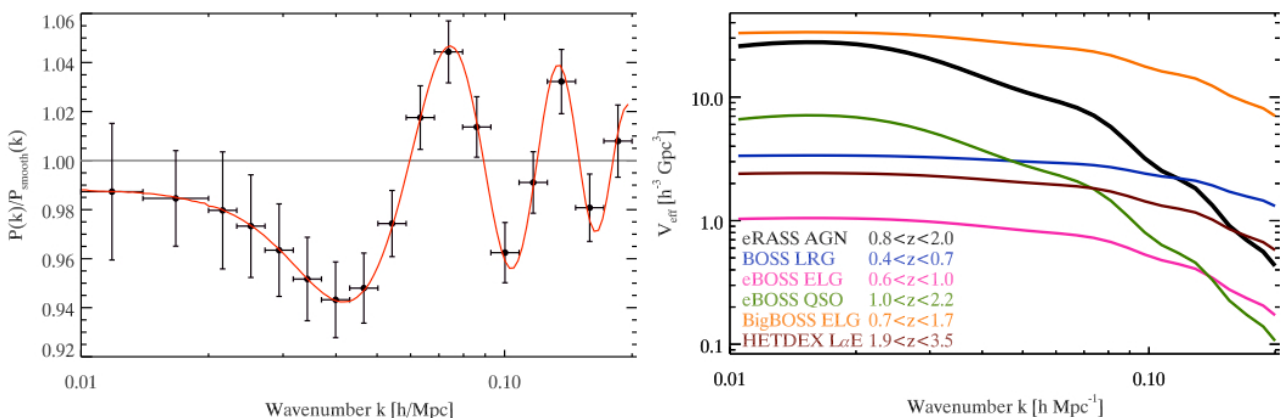
Left: BAO signal in the angular power spectra of eRASS AGN for the redshift interval z = 0–3, shown as residual with respect to a smooth broad-band spectral template. Error bars show statistical uncertainty in the angular power spectrum of the eRASS AGN. In this redshift range the BAO signal will be detected with a 14σ statistical confidence. Right: Effective volumes of various BAO surveys as a function of wavenumber computed for the redshift ranges indicated in the plot.

This capability is demonstrated in the left panel of the above Figure, where we show the total BAO signal, obtained by combining several narrow redshift slices between z=0.0 and 3.0. This will become the first measurement of BAOs with X-ray selected AGN sample. Moreover, a convincing

detection at the ~11σ level will become possible in the redshift range of z=0.8-2.0, currently uncovered by any of the existing BAO surveys. Although eRASS was never designed for BAO studies, it is remarkable that the statistical strength of its AGN sample is similar to those of dedicated BAO surveys. This can be seen in the right panel, where we show the effective volumes of BAO surveys as a function of wavenumber. This quantity is an indicator for the statistical performance of a galaxy clustering survey and the uncertainty of the power spectrum depends on it with $V_{eff}^{-0.5}$. Potentially, the eRASS AGN sample will become the best sample for BAO studies beyond redshift z>0.8 until the arrival of DESI (formerly known as BigBOSS) at the end of the decade. In order to realize this potential, comprehensive redshift measurements over large sky areas will be required.

References: Kolodzig et al. (2013a), A&A, 558, A89; Kolodzig et al. (2013b), A&A, 558, A90; Huetsi et al. (2014), A&A, 561, A58; Huetsi et al., (2014), in prep.

7. Recent bibliography

Scientific papers published since the last bulletin and mentioning "eROSITA" in their abstract in the period May 2013-January 2014 (from ADS):

- **Krumpe, Miyaji & Coil,** *Clustering Measurements of broad-line AGNs: Review and Future,* Refereed review article, paper is in print in Acta Polytechnica, 7 pages, 3 figures. eprint arXiv: 1308.5976
- **Brightman, et al**., *A statistical relation between the X-ray spectral index and Eddington ratio of active galactic nuclei in deep surveys,* MNRAS, 433, 2485
- **Kolodzig et al.,** *AGN and QSOs in the eROSITA All-Sky Survey. II. The large-scale structure.* A&A, 558, 90
- **Hajian, et al.,** *Measuring the thermal Sunyaev-Zel'dovich effect through the cross correlation of Planck and WMAP maps with ROSAT galaxy cluster catalogs*, JCAP, 11, 064
- **Schwope et al.,** *XMM-Newton observations of the low-luminosity cataclysmic variable V405 Pegasi,* A&A, 561, 121

8. Upcoming meetings and events

German eROSITA Consortium Meeting: AIP, Potsdam, September 15-17, 2014.

Meetings of General Interest (February 2014 - September 2014; from CADC):
- Matsuyama, Shikoku, Japan, February 19-22: *Suzaku-MAXI Conference 2014: Expanding the Frontiers of the X-ray Universe*
- La Thuile, Aosta Valley, Italy, March 22-29: *Rencontres de Moriond on Cosmology*
- Firenze, Italy, March 24-28: *The Structure and Signals of Neutron Stars, from Birth to Death*
- KITP, University of California, Santa Barbara, April 14-18: *Fire Down Below: The Impact of Feedback on Star and Galaxy Formation*
- Krakow, Poland, April 28- May 2: *The Evolving Blazar Paradigm*
- Dubrovnik, Croatia, May 12-16: *Multiwavelength-surveys: Galaxy formation and evolution from the early universe to today*
- Xi'an, China, May 18-23: *From dark matter to galaxies*
- Steigenberger Hotel Sanssouci, Potsdam, Germany, May 20-22: *COST conference "99 years of Black Holes - from Astronomy to Quantum Gravity"*

- Cefalu', Italy, June 2-13: *The Unquiet Universe: celebrating the 10th Anniversary of Astronomy Workshops in Cefalu' [Week One: The Distant Universe - Week Two: The Local Universe]*
- Bad Honnef, Germany, June 2-6: *The dance of stars: dense stellar systems from infant to old*
- Port Douglas, QLD, Australia, June 16-20: *Powerful AGN and Their Host Galaxies Across Cosmic Time*
- Moscow, Russia, June 16-20: *Cosmology and relativistic astrophysics (Zeldovich - 100)*
- Ierapetra, Crete, Greece, June 16-20: *Extreme Astrophysics in an Ever-Changing Universe - Time Domain Astronomy in the 21st Century | Celebrating John Seiradakis' 40-year career*
- Paris, France, June 16-19: *Gamma-Ray Bursts in the Multi-messenger Era*
- Dublin, Ireland, June 16-19: *XMM-Newton Conference: "The X-ray Universe 2014"*
- Montreal, Quebec - Canada, June 22-27: *SPIE Astronomical Telescopes + Instrumentation*
- Tallinn, Estonia, June 23-28: *The Zel'dovich' Universe - Genesis and Growth of the Cosmic Web*
- Paris, France, June 23-27: *Future Directions in Galaxy Cluster Surveys*
- Instituto de Fisica Teorica, Madrid, Spain, June 30-July 18: *nIFTy Cosmology: Numerical simulations for large surveys*
- Geneva, Switzerland, June 30- July 4: *EWASS 2014, Special Session 1: What powers Anomalous X-ray Pulsars and Soft Gamma-ray Repeaters?*
- European Southern Observatory, Garching, Germany, July 14-18: *Clustering Measurements of Active Galactic Nuclei*
- Near Innsbruck, Austria, July 21-25: *Alpine Cosmology workshop 2014*
- Durham, England, July 28- August 1: *AGN vs star formation: the fate of the gas in galaxies*
- Saint-Petersburg, Russia, July 28- August 1: *Physics of Neutron Stars - 2014*
- Moscow, Russia, August, 2-10: *40th Scientific Assembly of the Committee on Space Research (COSPAR 2014) and Associated Events*
- Chicago, Illinois, USA, August, 17-21: *High Energy Astrophysics Division of the AAS Meeting*
- Bamberg, Germany, September 22-27: *The variable sky: from tiny variations to big explosions, Annual meeting of the German Astronomical Society*